Arabian Journal for Science and Engineering (2019) 44:7013–7021
https://doi.org/10.1007/s13369-019-03754-5

RESEARCH ARTICLE - ELECTRICAL ENGINEERING

Decoupled Backstepping Sliding Mode Control of Underactuated Systems with Uncertainty: Experimental Results

Baris Ata[1] · Ramazan Coban[1]

Received: 26 July 2018 / Accepted: 2 February 2019 / Published online: 13 February 2019

Abstract
In this paper, a decoupled backstepping sliding mode control method is proposed to control underactuated systems under uncertainties and disturbances. The sliding mode control technique and the backstepping control technique are combined owing to their merits. Since the design methodology is based on the Lyapunov theorem, the stability of the system is guaranteed. The effectiveness of the proposed method is verified by the experimental results of the controller which is applied to a nonlinear, underactuated inverted pendulum system. The experimental results show that the decoupled backstepping sliding mode control achieves a satisfactory control performance rather than the decoupled sliding mode controller and the proposed method provides a robust performance to overcome parametric uncertainties where the decoupled sliding mode control fails.

Keywords Backstepping · Sliding mode · Decoupled sliding mode · Underactuated systems · Inverted pendulum on a cart

1 Introduction

Underactuated systems are mechanical systems with less number of actuators than their degrees of freedom. Consequently, they have at least one unactuated degree of freedom; hence, they consume less energy and their cost and complexity are low due to fewer actuators used in the systems. Because of these advantages, the control and analysis of underactuated mechanical systems have seen an enormous interest and active research in the last two decades [1–5]. However, the underactuated systems have nonholonomic constraints and they are not full-state feedback linearizable [6]. Therefore, controlling an underactuated mechanical system presents a challenging problem than the fully actuated systems. Hereby, a wide range of underactuated systems is used as benchmark tools to design and compare different control techniques, such as the beam and ball system, the translational oscillator with rotational actuator system and the inverted pendulum system [5,7,8].

The inverted pendulum is an underactuated system in which both angle and position are controlled by only one actuator. Also, other characteristics of the system such as nonlinearity and instability turn inverted pendulum into a challenging problem in the field of control engineering. Therefore, inverted pendulums have been classic tools in the control laboratories since the 1950s [9]. It is well known that the inverted pendulum system has two equilibrium point: One of them is stable and it corresponds to the downward position of the pendulum, and the other one is unstable and corresponds to the upright position of the pendulum. Therefore, maintaining the pendulum in the upright position using an appropriate continuous feedback signal can be considered as the main control problem [10]. Various techniques have been proposed to control an inverted pendulum, such as energy-based control [9,11,12], PID control [13,14], linear quadratic regulator [10] and sliding mode control (SMC) [4,15,16].

The SMC technique is a variable structure control method and it has been recognized as an effective robust control approach to model uncertainties and external disturbances [17,18]. The main aim of the SMC technique is to design a sliding surface to bring the system states there. The system can handle matched uncertainties and certain disturbances when the states reach the sliding surface [18]. Although the conventional SMC cannot be used directly on underactuated systems due to their coupled dynamics, the decoupled sliding mode control (DSMC) technique can be used to overcome this drawback [15]. The DSMC technique provides a method to decouple a nonlinear system into two subsystems

✉ Baris Ata
bata@cu.edu.tr

[1] Department of Computer Engineering, Cukurova University, Adana, Turkey

which have different control objectives. Using the DSMC method, the second subsystem can be incorporated into the first subsystem. Besides, the SMC can manage parametric uncertainties in combination with other methods such as backstepping control [19].

The backstepping technique is a nonlinear control method based on the Lyapunov theorem and also known as adding an integrator [20]. In the backstepping control, some of the states are used as virtual control signals in control law design, and the virtual signals satisfy the selected Lyapunov function in each step of the design process. Hence, the stability of the overall system can be guaranteed. The backstepping control design is mainly used to deal with the robust control of the nonlinear systems with parametric uncertainties [21]. Hereby, the SMC and the backstepping techniques can be combined to design a robust controller to uncertainties and disturbances [4,19,22]. The backstepping sliding mode control offers an improvement in steady-state error compared to the backstepping control and the SMC; also, it rejects disturbance and improves robustness against the parametric uncertainty [23].

In this study, both the backstepping control and the SMC techniques are combined and the decoupled backstepping sliding mode control (DBSMC) technique is proposed to control underactuated systems. The main objective of the DBSMC is to design a robust controller compared to DSMC when the system is subjected to parametric uncertainties. To demonstrate the performance and effectiveness of the proposed method, a decoupled backstepping sliding mode controller has been experimentally applied to an inverted pendulum on a cart system. The rest of the paper is organized as follows. In Sect. 2, the problem formulation is presented. The DBSMC method is explained and a decoupled backstepping sliding mode controller is designed in Sect. 3. Experimental results and the conclusion of the study are presented in Sects. 4 and 5, respectively.

2 Problem Formulation

In this study, a digital pendulum mechanical unit is used to perform experiments. The pendulum mechanical unit consists of an inverted pendulum hinged on a cart and a belt mechanism with a DC motor on adjustable foot. The pendulum angle and the cart position signals are transferred to the digital pendulum controller and then to the PC, where the control algorithm is placed. The experimental setup of the inverted pendulum on a cart is presented in Fig. 1.

The inverted pendulum system consists of a cart moving along a rail and a rod which is hinged to cart as shown in Fig. 2. Let x be the displacement of the cart from the initial position and θ is the angle in the vertical direction. Hence,

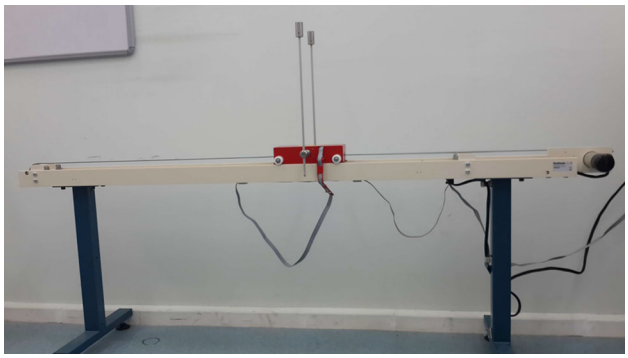

Fig. 1 Inverted pendulum on a cart system

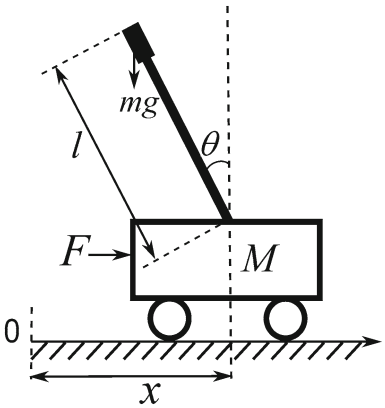

Fig. 2 Parametric representation of the inverted pendulum

the equation of motions in both translational motion and rotational motion can be written as follows, respectively [24]:

$$\begin{aligned}\ddot{x} &= \frac{-(J_p + ml^2)b\dot{x} + m^2l^2g\cos(\theta)\sin(\theta)}{\Gamma} \\ &\quad - \frac{ml\cos(\theta)d\dot{\theta} + (J_p + ml^2)ml\dot{\theta}^2\sin(\theta)}{\Gamma} \\ &\quad + \frac{(J_p + ml^2)F}{\Gamma} \end{aligned} \tag{1}$$

$$\begin{aligned}\ddot{\theta} &= \frac{(M+m)mgl\sin(\theta) - m^2l^2\cos(\theta)\sin(\theta)\dot{\theta}^2}{\Gamma} \\ &\quad - \frac{mlb\cos(\theta)\dot{x} + (M+m)d\dot{\theta} - ml\cos(\theta)F}{\Gamma}, \end{aligned} \tag{2}$$

where $\Gamma = (J_p + ml^2)(M+m) - m^2l^2\cos^2(\theta)$. And also, m and l are the mass and the length of the pendulum, respectively; M is the mass of the cart; J_p is the moment of inertia; d is the pendulum damping coefficient; g is the acceleration due to gravity; F is the force applied to the cart; and b is the cart friction coefficient. The inverted pendulum parameters are presented in Table 1.

The cart of the inverted pendulum system is driven by a DC motor. The motor characteristics should be added to the

Table 1 Parameters of the inverted pendulum [26]

Parameter	Value
M	2.3 kg
m	0.2 kg
l	0.3 m
g	9.81 m/s^2
J_p	0.009 kgm^2
d	0.005 Nms/rad
b	0.00005 Ns/m

Table 2 Parameters of the DC motor [24]

Parameter	Value
R	2.5 Ω
r	0.0314 m
K_t	0.05
K_b	0.05
n_1	18.84
n_2	0.986

inverted pendulum model to design a more realistic system. Therefore, a differential equation for electromechanical signal conversion from voltage $e(t)$ to force $F(t)$ can be written as follows [23]:

$$F(t) = -\left(\frac{n_1}{r}\right)\left(\frac{n_2}{r}\right)\frac{K_b K_t}{R}\dot{x}(t) + \left(\frac{n_1}{r}\right)\frac{K_t}{R}e(t), \tag{3}$$

where R is the rotor circuit resistance; K_t is the torque constant; and K_b is the backelectromotive force constant. Also n_1 and n_2 are gear ratios and r is the pulley radius. The DC motor parameters are presented in Table 2.

Taking the states as $[x_1\ x_2\ x_3\ x_4] = [x\ \dot{x}\ \theta\ \dot{\theta}]$ and substituting Eq. 3 into Eqs. 1 and 2, the state equations of the inverted pendulum can be written as follows:

$$\begin{aligned}
\dot{x}_1 &= x_2\\
\dot{x}_2 &= \frac{\delta_1\left(\phi x_2 + \varphi\cos(x_3)\sin(x_3) + \gamma\sin(x_3)x_4^2\right)}{\psi - \rho\cos^2(x_3)}\\
&\quad + \frac{\delta_1\eta\cos(x_3)x_4 + \lambda u}{\psi - \rho\cos^2(x_3)} + \xi_1(t)\\
\dot{x}_3 &= x_4\\
\dot{x}_4 &= \frac{\delta_2\left(\mu x_2\cos(x_3) + \vartheta\sin(x_3) + \sigma x_4\right)}{\psi - \rho\cos^2(x_3)}\\
&\quad + \frac{\delta_2\rho\cos(x_3)\sin(x_3)x_4^2 + \tau\cos(x_3)u}{\psi - \rho\cos^2(x_3)} + \xi_2(t),
\end{aligned} \tag{4}$$

where

$$\begin{aligned}
\phi &= -(J_\mathrm{p} + ml^2)\left(b + \left(n_1/r\right)\left(n_2/r\right)\left(K_b K_t/R\right)\right)\\
\varphi &= m^2 l^2 g\\
\gamma &= -(J_\mathrm{p} + ml^2)ml\\
\eta &= -mld\\
\lambda &= (J_\mathrm{p} + ml^2)\left(\left(n_1/r\right)\left(K_t/R\right)\right)\\
\mu &= -ml\left(b + \left(n_1/r\right)\left(n_2/r\right)\left(K_b K_t/R\right)\right)\\
\vartheta &= (M+m)mgl\\
\rho &= m^2 l^2\\
\sigma &= (M+m)d\\
\tau &= ml\left(\left(n_1/r\right)\left(K_t/R\right)\right)\\
\psi &= (J_\mathrm{p} + ml^2)(M+m);
\end{aligned}$$

δ_1 and δ_2 stand for the parametric uncertainties as constants; $\xi_1(t)$ and $\xi_2(t)$ are the total amounts of external disturbances and unmatched uncertainties. $\xi_1(t)$ and $\xi_2(t)$ are assumed to be bounded as $|\xi_1(t)| \le \xi_{1\,\max}$ and $|\xi_2(t)| \le \xi_{2\,\max}$.

3 Design Methods

Dynamical equations of a general single-input single-output nonlinear system can be described by

$$\begin{aligned}
\dot{x}_1(t) &= x_2(t)\\
\dot{x}_2(t) &= \delta f(x) + g(x)u(t) + \xi(t)\\
y(t) &= x_1(t),
\end{aligned} \tag{5}$$

where $f(x)$ and $g(x)$ are nonlinear functions, $x = [x_1, x_2]^T$ is the state vector, δ is the parametric uncertainty, $\xi(t)$ is the total amounts of external disturbances and unmatched uncertainties, $y(t)$ is the output and $u(t)$ is the control input. In order to design a sliding mode controller for this system, a sliding surface can be defined as

$$s(t) = k_1 e(t) + \dot{e}(t) \tag{6}$$

using the tracking error

$$e(t) = y(t) - y_\mathrm{d}, \tag{7}$$

where $k_1$is a real positive constant and y_d is the desired output.

Considering a Lyapunov function

$$V(s) = \frac{1}{2}s^2(t) \tag{8}$$

and differentiating $V(s)$ yield

$$\begin{aligned}\dot{V}(s) &= s(t)\dot{s}(t)\\ &= s(t)(k_1\dot{e}(t)+\ddot{e}(t))\\ &= s(t)\left(k_1\dot{e}(t)+\delta f(x)+g(x)u(t)+\xi(t)\right).\end{aligned} \tag{9}$$

$\dot{V}(s)$ in Eq. 9 will be negative definite if the control law is defined as

$$u(t) = u_{\text{eq}}(t) + u_{\text{sw}} \tag{10}$$

with

$$u_{\text{eq}}(t) = \frac{1}{g(x)}\left(-k_1\dot{e}(t) - \delta f(x)\right), \tag{11}$$

$$u_{\text{sw}}(t) = -\frac{1}{g(x)}K\,\text{sign}\left(s(t)\right), \tag{12}$$

and

$$\text{sign}(s(t)) = \begin{cases} 1, & s(t) > 0\\ 0, & s(t) = 0\\ -1, & s(t) < 0\end{cases} \tag{13}$$

where $K \geq \xi_{\max}$. Substituting Eq. 10 into Eq. 9 yields

$$\begin{aligned}\dot{V}(s) &= s(t)\left[k_1\dot{e}(t)+\delta f(x)\right]\\ &\quad + s(t)\left[g(x)\left(u_{\text{eq}}(t)+u_{\text{sw}}(t)\right)+\xi(t)\right].\end{aligned} \tag{14}$$

Substituting Eqs. 11 and 12 into Eq. 14, one has

$$\begin{aligned}\dot{V}(s) &= -Ks(t)\text{sign}\left(s(t)\right)\\ &= -K\left|s(t)\right| \leq 0.\end{aligned} \tag{15}$$

According to the Lyapunov theorem, due to the fact that $\dot{V}(s)$ is negative definite, the system trajectory will be driven to sliding surface and remain there until the origin is reached asymptotically.

Using sign $(s(t))$ function will lead the chattering. A boundary level with width Δ can be defined. and sign $(s(t))$ function can be replaced with a saturation function in Eq. 12 to overcome this problem as follows:

$$u_{\text{sw}}(t) = -\frac{1}{g(x)}K\,\text{sat}\left(s(t)/\Delta\right) \tag{16}$$

with

$$\text{sat}(\Gamma) = \begin{cases} \text{sign}(\Gamma), & |\Gamma| \geq 1\\ \Gamma, & |\Gamma| < 1\end{cases} \tag{17}$$

where $\Delta > 0$.

The SMC design can be applied to systems presented in the canonical form. Nevertheless, the dynamic representation of the inverted pendulum on a cart system presented in Eq. 4 has a form shown as follows rather than the canonical form

$$\begin{aligned}\dot{x}_1(t) &= x_2(t)\\ \dot{x}_2(t) &= \delta_1 f_1(x) + g_1(x)u(t) + \xi_1(t)\\ \dot{x}_3(t) &= x_4(t)\\ \dot{x}_4(t) &= \delta_2 f_2(x) + g_2(x)u(t) + \xi_2(t),\end{aligned} \tag{18}$$

where $x = [x_1, x_2, x_3, x_4]^T$ is the state vector; $f_1(x)$, $g_1(x)$, $f_2(x)$ and $g_2(x)$ are nonlinear functions; $u(t)$ is the control input; $\delta_1$and δ_2 are the parametric uncertainties as constants; and $\xi_1(t)$ and $\xi_2(t)$ are the total amounts of external disturbances and unmatched uncertainties. $\xi_1(t)$ and $\xi_2(t)$ are assumed to be bounded as $|\xi_1(t)| \leq \xi_{1\max}$ and $|\xi_2(t)| \leq \xi_{2\max}$.

The decoupled control idea can be used to design a controller to control both the displacement and the angle in the inverted pendulum on a cart system. The main idea behind the decoupled sliding mode control is to decouple the whole system into two subsystems and define a sliding surface for each subsystem. The control objective of a sliding mode controller is to drive the sliding surface to zero; hence, using an intermediate variable to transfer value from a sliding surface to the other can lead to control both subsystems simultaneously. To design a decoupled sliding mode controller for this system, two different sliding surfaces can be defined as follows [15,25]:

$$s_{S1}(t) = k_1 e_1(t) + \dot{e}_1(t) \tag{19}$$

$$s_{S2}(t) = k_2 e_2(t) + \dot{e}_2(t), \tag{20}$$

where k_1 and k_2 are real positive constants, and $e_1(t)$ and $e_2(t)$ are tracking errors for the cart displacement and pendulum angle, respectively. $s_{S2}(t)$ in Eq. 20 can be transformed to a decoupled sliding surface as

$$s_{S2}(t) = k_2(e_2(t) - z_{\text{S}}) + \dot{e}_2(t) \tag{21}$$

with z_{S} is a value transferred from s_{S1} and defined as

$$z_{\text{S}} = \text{sat}(s_{S1}(t)/\Delta_{\text{Sz}})z_{\text{Su}}, \quad 0 < z_{\text{Su}} < 1, \tag{22}$$

where z_{Su} is the upper bound of z_{S} and Δ_{Sz} is the boundary level as constants. z_{Su}, the upper bound of the intermediate variable z_{S}, guarantees that $s_{S2}(t)$ will be limited. After the sliding surface $s_{S1}(t)$ becomes zero, $s_{S2}(t)$ will be driven to zero too, thanks to z_{S}.

According to Eq. 10, the decoupled sliding mode controller to move the cart to a desired position while maintaining the pendulum at the upright position can be defined as follows:

$$\begin{aligned} u_{\mathrm{S}}(t) &= u_{\mathrm{Seq}} + u_{\mathrm{Ssw}} \\ &= \frac{1}{g_2(x)}\left(-k_2\dot{e}_2(t) - \delta_2 f_2(x)\right) \\ &\quad - \frac{1}{g_2(x)}(K_{\mathrm{S}}\mathrm{sign}(s_{S2}(t)), \end{aligned} \tag{23}$$

where $K_{\mathrm{S}} \geq \xi_{2\max}$.

Therewith, a decoupled sliding mode controller for the inverted pendulum on a cart system introduced in Eq. 4 can be defined by

$$\begin{aligned} s_{S1}(t) &= k_1 e_1(t) + \dot{e}_1(t) \\ s_{S2}(t) &= k_2\left(e_2(t) - z\right) + \dot{e}_2(t) \\ u_{\mathrm{S}}(t) &= \frac{1}{g_2(x)}\left(-k_2\dot{e}_2(t) - \delta_2 f_2(x)\right) \\ &\quad - \frac{1}{g_2(x)}(K_{\mathrm{S}}\mathrm{sign}(s_{S2}(t)), \end{aligned} \tag{24}$$

where

$$\begin{aligned} f_2(x) &= \frac{\mu x_2\cos(x_3) + \vartheta\sin(x_3)}{\psi - \rho\cos^2(x_3)} \\ &\quad + \frac{\rho\cos(x_3)\sin(x_3)x_4^2 + \sigma x_4}{\psi - \rho\cos^2(x_3)} \\ g_2(x) &= \frac{\tau\cos(x_3)}{\psi - \rho\cos^2(x_3)}. \end{aligned} \tag{25}$$

The sliding mode control can handle any kind of matched uncertainties; however, it has a deficiency to handle parametric uncertainties. In order to manage this drawback, both the backstepping control and SMC techniques can be combined. The steps of the backstepping sliding mode control (BSMC) can be designed as follows.

Let the tracking error $e(t)$ be defined as in Eq. 7. The derivative of the error can be presented as

$$\dot{e}(t) = \dot{x}_1(t) - \dot{y}_{\mathrm{d}} = x_2(t) - \dot{y}_{\mathrm{d}}. \tag{26}$$

Consider a Lyapunov function

$$V_{B1}(e) = \frac{1}{2}e^2(t) \tag{27}$$

which is positive definite by the definition. Time derivative of $V_{B1}(e)$ is obtained as follows:

$$\dot{V}_{B1}(e) = e(t)\dot{e}(t) = e(t)\left(x_2(t) - \dot{y}_{\mathrm{d}}\right). \tag{28}$$

Letting $x_2(t) = s_B(t) - b_1 e(t) + \dot{y}_{\mathrm{d}}$ as a virtual control and rearranging Eq. 28 yields

$$\dot{V}_{B1}(e) = e(t)s_B(t) - b_1 e^2(t), b_1 > 0, \tag{29}$$

where the sliding variable $s_B(t) = x_2(t) + b_1 e(t) - \dot{y}_{\mathrm{d}}$. $\dot{V}_{B1}(e) = -b_1 e^2 < 0$ for $s_B = 0$; therefore, $\dot{V}_{B1}(e)$ is negative definite. To design a backstepping controller, the next step is required.

Selecting the second Lyapunov function as

$$V_{B2}(e) = V_{B1}(e) + \frac{1}{2}{s_B}^2(t) \tag{30}$$

and with the help of Eq. 5 time derivative of the Lyapunov function in Eq. 30 yields

$$\begin{aligned} \dot{V}_{B2}(e) &= \dot{V}_{B1}(e) + s_B(t)\dot{s}_B(t) \\ &= \dot{V}_{B1}(e) + s_B(t)\left[\delta f(x) + g(x)u_B(t)\right] \\ &\quad + s_B(t)\left[\xi(t) + b_1\dot{e}(t) - \ddot{y}_{\mathrm{d}}\right]. \end{aligned} \tag{31}$$

In order to realize that $\dot{V}_{B2}(e)$ is negative definite, the backstepping controller law can be designed as follows:

$$\begin{aligned} u_{\mathrm{Beq}}(t) &= \frac{1}{g(x)}\left[-\delta f(x) - e(t)\right] \\ &\quad + \frac{1}{g(x)}\left[-b_1\dot{e}(t) + \ddot{y}_{\mathrm{d}} - b_2 s(t)\right], \end{aligned} \tag{32}$$

where b_1 and b_2 are positive constants. Hence, $\dot{V}_{B2}(e)$ becomes

$$\dot{V}_{B2}(e) = -b_1 e^2(t) - b_2 {s_B}^2(t) + \xi(t)s_B(t). \tag{33}$$

To guarantee the stability of the system, a switching control law can be defined as follows:

$$u_{\mathrm{Bsw}}(t) = -\frac{1}{g(x)}B\mathrm{sign}(s_B(t)). \tag{34}$$

Putting the control laws in Eqs. 32 and 33 together gives the robust control law known as backstepping sliding mode control which can be defined as

$$\begin{aligned} u_B(t) &= \frac{1}{g(x)}\left[-\delta f(x) - e(t) - b_1\dot{e}(t) + \ddot{y}_{\mathrm{d}}\right] \\ &\quad + \frac{1}{g(x)}\left[-b_2 s(t) - B\mathrm{sign}\left(s_B(t)\right)\right]. \end{aligned} \tag{35}$$

With the help of Eq. 34, the time derivative of the Lyapunov function in Eq. 30 can be rewritten as

$$\begin{aligned} \dot{V}_{B2}(e) &= -b_1 e^2(t) - b_2 {s_B}^2(t) + \xi(t)s_B(t) \\ &\quad - B\left|s_B(t)\right| < 0, \end{aligned} \tag{36}$$

where $B \geq \xi_{\max} \geq |\xi(t)|$. Since $\dot{V}_{B2}(e)$ is negative definite, the system trajectory will be driven to sliding surface and remain there until the origin is reached asymptotically. Consequently, the stability of the overall system is guaranteed.

The BSMC technique can be applied to systems presented in the canonical form as in SMC. However, using the presented BSMC method, a decoupled backstepping sliding mode controller can be designed for the inverted pendulum on a cart system. To this end, defining the tracking errors e_1 for the cart displacement and e_2 for the pendulum angle as

$$\begin{aligned} e_1(t) &= x_1(t) - y_{d1} \\ e_2(t) &= x_3(t) - y_{d2} \end{aligned} \tag{37}$$

and time-derivating them result in

$$\begin{aligned} \dot{e}_1(t) &= \dot{x}_1(t) - \dot{y}_{d1} = x_2(t) - \dot{y}_{d1} \\ \dot{e}_2(t) &= \dot{x}_3(t) - \dot{y}_{d2} = x_4(t) - \dot{y}_{d2}. \end{aligned} \tag{38}$$

Considering a Lyapunov function candidate

$$V_{D1}(e) = \frac{1}{2} {e_2}^2(t) \tag{39}$$

and differentiating it result in

$$\dot{V}_{D1}(e) = e_2(t)\dot{e}_2(t) = e_2(t)\left(x_4(t) - y_{d2}\right). \tag{40}$$

In this step of the DBSMC design, two different sliding surfaces can be chosen unlike the BSMC

$$\begin{aligned} s_{D1}(t) &= c_1 e_1(t) + \dot{e}_1(t) \\ s_{D2}(t) &= c_2 e_2(t) + \dot{e}_2(t), \end{aligned} \tag{41}$$

where c_1 and c_2 are real positive constants.

Letting $x_4(t) = s_{D2}(t) - c_2 e_2(t) + \dot{y}_{d2}$ from s_{D2} in Eq. 41 and substituting it into Eq. 40, one has

$$\dot{V}_{D1}(e) = e_2(t) s_{D2}(t) - c_2 {e_2}^2. \tag{42}$$

$\dot{V}_{D1}(e) = -c_2 {e_2}^2(t)$ will be negative definite, if only $s_{D2}(t) = 0$. Therefore, in order to ensure the stability of the DBSMC, the Lyapunov function for the next step can be chosen as follows:

$$V_{D2}(e) = V_{D1}(e) + \frac{1}{2} s_{\mathrm{D}2}^2(t). \tag{43}$$

Using Eq. 18, the time derivative of Eq. 43 is

$$\begin{aligned} \dot{V}_{D2}(e) &= \dot{V}_{D1}(e) + s_{D2}(t)\dot{s}_{D2}(t) \\ &= e_2(t) s_{D2}(t) - c_2 {e_2}^2(t) \\ &\quad + s_{D2}(t)\left(\delta_2 f_2(x) + g_2(x) u_{\mathrm{D}}(t)\right) \\ &\quad + s_{D2}(t)\left(\xi(t) + c_2\dot{e}_2(t) - \ddot{y}_{d2}\right). \end{aligned} \tag{44}$$

In order to ensure $\dot{V}_{D2}(e)$ is negative definite, the decoupled backstepping control law can be chosen as

$$\begin{aligned} u_{\mathrm{Deq}}(t) &= \frac{1}{g_2(x)}\left(-\delta_2 f_2(x) - e_2(t) - c_2\dot{e}_2(t)\right) \\ &\quad + \frac{1}{g_2(x)}\left(\ddot{y}_{d2} - c_3 s_{D2}(t)\right), \end{aligned} \tag{45}$$

where c_3 is a real positive constant. To ensure the stability of the system, a switching control law can be defined as follows:

$$u_{\mathrm{Dsw}}(t) = -\frac{1}{g_2(x)} C \,\mathrm{sign}(s_{D2}(t)), \tag{46}$$

where C is a real positive constant.

The control law $u_{\mathrm{D}}(t)$ can be defined as putting the control laws in Eqs. 45 and 46 together

$$u_{\mathrm{D}}(t) = u_{\mathrm{Deq}}(t) + u_{\mathrm{Dsw}}(t). \tag{47}$$

Substitution of (47) into (44) results in

$$\begin{aligned} \dot{V}_{D2}(e) &= -c_2 {e_2}^2(t) - c_3 s_{\mathrm{D}2}^2(t) + \xi_2(t) s_{D2}(t) \\ &\quad - C\left|s_{D2}(t)\right|. \end{aligned} \tag{48}$$

The time derivative of the Lyapunov function $\dot{V}_{D2}$ will be negative definite where $C \geq \xi_{2\max} \geq |\xi_2(t)|$.

To create a decoupled controller, a virtual sliding surface s_{d} can be considered as

$$s_{\mathrm{d}}(t) = c_2(e_2(t) - z_{\mathrm{D}}) + \dot{e}_2(t) \tag{49}$$

with z_{D} is a value transferred from s_{D1} and defined as

$$z_{\mathrm{D}}(t) = \mathrm{sat}\left(s_{D1}(t)/\Delta_{\mathrm{Dz}}\right) z_{\mathrm{Du}}, 0 < z_{\mathrm{Du}} < 1, \tag{50}$$

where z_{Du}, the upper bound of the $z_{\mathrm{D}}(t)$, guarantees that $s_{\mathrm{d}}(t)$ will be limited.

Consequently, substituting $s_{\mathrm{d}}(t)$ in Eq. 49 into Eq. 47 for $s_{D2}(t)$ gives the DBSMC control law

$$\begin{aligned} u_{\mathrm{D}}(t) &= \frac{1}{g_2(x)}\left(-\delta_2 f_2(x) - e_2(t) - c_2\dot{e}_2(t)\right) \\ &\quad + \frac{1}{g_2(x)}\left(\ddot{y}_{d2} - c_3 s_{\mathrm{d}}(t)\right) \\ &\quad - \frac{1}{g_2(x)} C \,\mathrm{sign}(s_{\mathrm{d}}(t)), \end{aligned} \tag{51}$$

where

$$\begin{aligned} f_2(x) &= \frac{\mu x_2 \cos(x_3) + \vartheta \sin(x_3)}{\psi - \rho\cos^2(x_3)} \\ &\quad + \frac{\rho \cos(x_3)\sin(x_3) x_4^2 + \sigma x_4}{\psi - \rho\cos^2(x_3)} \\ g_2(x) &= \frac{\tau \cos(x_3)}{\psi - \rho\cos^2(x_3)}. \end{aligned}$$

4 Experimental Results

In order to evaluate the performance of the proposed DBSMC, it is applied to the inverted pendulum on a cart system in Eq. 4 having the parameters given in Tables 1 and 2. The block diagram of the DBSMC is presented in Fig. 3.

The goals of these experimental tests are to show the changes on the position of the cart $x(t)$, the pendulum angle $\theta(t)$ and the control signal $u(t)$ based on initial conditions of $\left[\, x_0 \; \dot{x}_0 \; \theta_0 \; \dot{\theta}_0 \,\right]^T$ and reference signal y_d, using the DSMC presented in Eq. 24 and the DBSMC introduced in Eq. 51 on the experimental setup. The sat function in Eq. 17 instead of sign function is employed in the switching controls $u_{\mathrm{Ssw}}(t)$ and $u_{\mathrm{Dsw}}(t)$ due to decrease the chattering. Parametric uncertainties which can result from errors in the measurement of parameters are defined as δ_2. No external perturbation is injected to the system during the experiments, and own external disturbances of the inverted pendulum on a cart system can be compensated by the DSMC and the DBSMC. The experimental setup has two physical constraints. The first one is the cart position which is physically bounded by the rail length which is 0.8 m. Since it is assumed that the initial cart position is in the middle of the rail, position of the cart should be limited to $|x| \leq 0.4$ m. Therefore, the controllers are designed to limit the maximum displacement of the cart to ± 0.35 m. The second constraint is the bound of the control signal which must be in the range of -2.5 V and $+2.5$ V [26]. The DSMC and the DBSMC parameters which are chosen by trial and error method with considering these constraints are given in Table 3. The control problem is chosen as moving the cart to the desired position while stabilizing the pendulum at the upright position. For all experiments, a step reference of 0.3 m is applied to the control system and also the initial conditions of the system are chosen as $\left[\, x_0 \; \dot{x}_0 \; \theta_0 \; \dot{\theta}_0 \,\right]^T = \left[\, 0 \; 0 \; 0.1 \; 0 \,\right]^T$.

In the first experiment, both the DSMC and the DBSMC are applied to the inverted pendulum on a cart system with the parametric uncertainty $\delta_2 = 1$. Thus, the control methods are tested on own parametric uncertainties of the system without any additional parametric uncertainty. For comparison purpose, the test results of the cart position, pendulum angle and control signal are plotted and shown in Fig. 4a–c, respectively. The settling time and steady-state errors are about 4 s and 0.012 m for the DSMC and 4.1 s and 0 m for the DBSMC, respectively. Both the DSMC and the DBSMC manage to bring the cart from the initial position to the desired position as shown in Fig. 4a. However, the DBMS has a much better performance to stabilize the position. Figure 4b clearly shows that the both controllers are able to keep the pendulum on the upright position. The chattering in the control signal is slightly lower in the DSMC as compared the DBSMC as shown in Fig. 4c.

In the second experiment, the parametric uncertainty $\delta_2 = 0.8$ is applied to the inverted pendulum on a cart system.

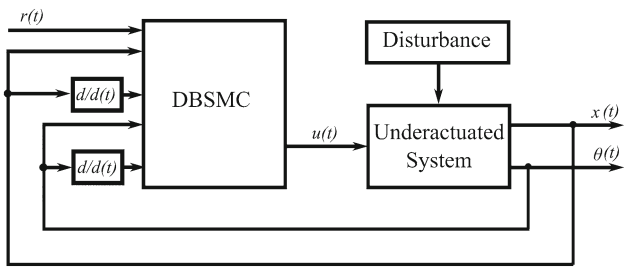

Fig. 3 Block diagram of the DBSMC

Table 3 Parameters of controllers

Parameter	Value
k_1, c_1	1
k_2, c_2	40
c_3	10
K_S, B	30
$z_{\mathrm{Su}}, z_{\mathrm{Du}}$	0.97
$\Delta_{\mathrm{Sz}}, \Delta_{\mathrm{Dz}}$	6
Δ	5

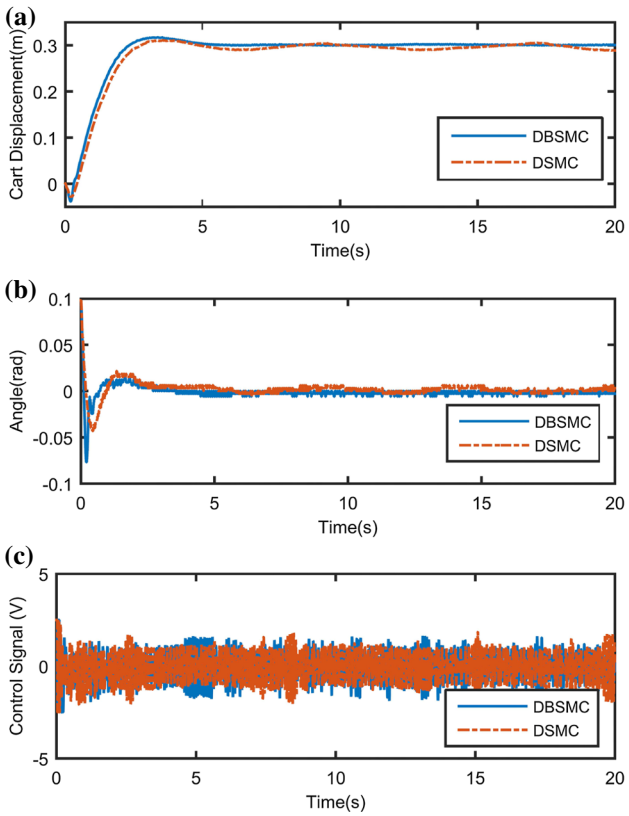

Fig. 4 Experimental results with the matched uncertainty for $\delta_2 = 1$: **a** displacement of the cart, **b** angular displacement of the pendulum, **c** control input

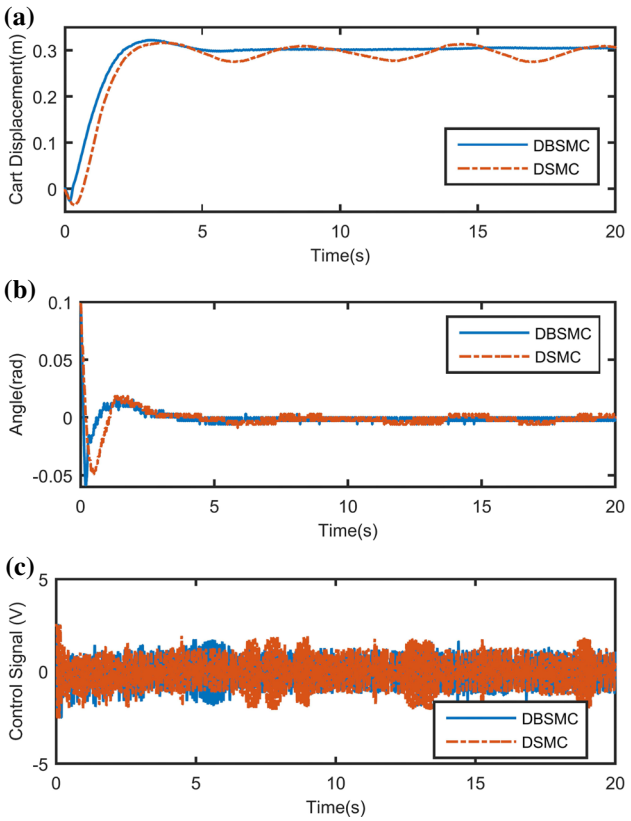

Fig. 5 Experimental results with the matched uncertainty for $\delta_2 = 0.8$: **a** displacement of the cart, **b** angular displacement of the pendulum, **c** control input

Although the DSMC is able to bring and keep the pendulum at the upright position, it fails to stabilize the cart at the desired position as shown in Fig. 5a, b. On the other hand, the DBSMC manages to handle the parametric uncertainty and control the cart position successfully with 4.4 s settling time and 0.005 m steady-state error. Besides, the DBSMC yields slightly lower chattering in the control signal compared to the DSMC as shown in Fig. 5c.

5 Conclusion

In this paper, a decoupled backstepping sliding mode control (DBSMC) method is proposed to control underactuated systems. The proposed DBSMC keeps the advantages of the sliding mode control and overcomes the difficulties caused by the parametric uncertainties. In order to confirm the effectiveness of the proposed DBSMC, it is applied to an inverted pendulum on a cart system as a benchmark example for underactuated systems. The experimental results show that the DBSMC is more effective compared to the decoupled sliding mode control (DSMC). Also, the experimental results prove that the DBSMC provides a robust control on the systems with parametric uncertainties where the DSMC fails. This study provides a basis for the application of the DBSMC to the underactuated systems. Future research should consider the potential of the DBSMC method on different underactuated systems. Also, adding an adaptive scheme to the DBSMC might prove an important area for future research.

References

1. Spong, M.W.: Underactuated Mechanical Systems. Control Problems in Robotics and Automation, pp. 135–150. Springer, London (1998). https://doi.org/10.1007/BFb0015081
2. Man, W.; Lin, J.S.: Nonlinear control design for a class of underactuated systems. In: 2010 IEEE International Conference on Control Applications pp. 1439–1444 (2010). https://doi.org/10.1109/CCA.2010.5611126
3. Chen, Y.F.; Huang, A.C.: Controller design for a class of underactuated mechanical systems. IET Control Theory Appl. **6**(1), 103 (2012). https://doi.org/10.1049/iet-cta.2010.0667
4. Adhikary, N.; Mahanta, C.: Integral backstepping sliding mode control for underactuated systems: swing-up and stabilization of the cart-pendulum system. ISA Trans. **52**(6), 870–880 (2013). https://doi.org/10.1016/j.isatra.2013.07.012
5. Shah, I.; Rehman, F.U.: Smooth second order sliding mode control of a class of underactuated mechanical systems. IEEE Access **6**(c), 7759–7771 (2018). https://doi.org/10.1109/ACCESS.2018.2806568
6. Isidori, A.: Nonlinear Control Systems. Communications and Control Engineering. Springer, London (1995). https://doi.org/10.1007/978-1-84628-615-5
7. She, J.; Zhang, A.; Lai, X.; Wu, M.: Global stabilization of 2-DOF underactuated mechanical systems-an equivalent-input-disturbance approach. Nonlinear Dyn. **69**(1–2), 495–509 (2012). https://doi.org/10.1007/s11071-011-0280-3
8. Zhang, A.; Lai, X.; Wu, M.; She, J.: Nonlinear stabilizing control for a class of underactuated mechanical systems with multi degree of freedoms. Nonlinear Dyn. **89**(3), 2241–2253 (2017). https://doi.org/10.1007/s11071-017-3582-2
9. Åström, K.J.; Furuta, K.: Swinging up a pendulum by energy control. Automatica **36**(2), 287–295 (2000). https://doi.org/10.1016/S0005-1098(99)00140-5
10. Ata, B.; Coban, R.: Artificial bee colony algorithm based linear quadratic optimal controller design for a nonlinear inverted pendulum. Int. J. Intell. Syst. Appl. Eng. **3**(1), 1 (2015). https://doi.org/10.18201/ijisae.87020
11. Spong, M.W.: Energy based control of a class of underactuated mechanical systems. IFAC Proc Volumes **29**(1), 2828–2832 (1996). https://doi.org/10.1016/S1474-6670(17)58105-7
12. Siuka, A.; Schöberl, M.: Applications of energy based control methods for the inverted pendulum on a cart. Robot. Auton. Syst. **57**(10), 1012–1017 (2009). https://doi.org/10.1016/J.ROBOT.2009.07.016
13. Chang, W.D.; Hwang, R.C.; Hsieh, J.G.: A self-tuning PID control for a class of nonlinear systems based on the Lyapunov approach. J. Process Control **12**(2), 233–242 (2002). https://doi.org/10.1016/S0959-1524(01)00041-5
14. Subudhi, B.; Ghosh, A.; Krishnan, T.: Robust proportional-integral-derivative compensation of an inverted cart-pendulum system: an experimental study. IET Control Theory Appl. **6**(8), 1145–1152 (2012). https://doi.org/10.1049/iet-cta.2011.0251

15. Lo, J.-C.; Kuo, Y.-H.: Decoupled fuzzy sliding-mode control. IEEE Trans. Fuzzy Syst. **6**(3), 426–435 (1998). https://doi.org/10.1109/91.705510
16. Mahjoub, S.; Mnif, F.; Derbel, N.: Second-order sliding mode approaches for the control of a class of underactuated systems. Int. J. Autom. Comput. **12**(2), 134–141 (2015). https://doi.org/10.1007/s11633-015-0880-3
17. Utkin, V.: Variable structure systems with sliding modes. IEEE Trans. Autom. Control **22**(2), 212–222 (1977). https://doi.org/10.1109/TAC.1977.1101446
18. Utkin, V.: Sliding Modes in Control and Optimization. Springer, Berlin (1992). https://doi.org/10.1007/978-3-642-84379-2
19. Coban, R.: Backstepping integral sliding mode control of an electromechanical system. Automatika **58**(3), 266–272 (2018). https://doi.org/10.1080/00051144.2018.1426263
20. Freeman, R.A.; Kokotovic, P.: Robust Nonlinear Control Design: State-Space and Lyapunov Techniques. Birkhäuser, Boston (1996)
21. Wang, Q.; Stengel, R.F.: Robust control of nonlinear systems with parametric uncertainty. Automatica **38**, 1591 –1599 (2002)
22. Lu, C.H.; Hwang, Y.R.; Shen, Y.T.: Backstepping sliding mode tracking control of a vane-type air motor X-Y table motion system. ISA Trans. **50**(2), 278–286 (2011). https://doi.org/10.1016/J.ISATRA.2010.12.008
23. Coban, R.: Backstepping sliding mode tracking controller design and experimental application to an electromechanical system. J. Control Eng. Appl. Inform. **19**(3), 88–96 (2017)
24. Ata, B.; Coban, R.: Linear quadratic optimal control of an inverted pendulum on a cart using artificial bee colony algorithm: an experimental study. Cukurova Univ. J. Fac. Eng. Archit. **32**(2), 109–124 (2017). https://doi.org/10.21605/cukurovaummfd.358391
25. Coban, R.; Ata, B.: Decoupled sliding mode control of an inverted pendulum on a cart: an experimental study. In: IEEE/ASME International Conference on Advanced Intelligent Mechatronics, AIM (2017). https://doi.org/10.1109/AIM.2017.8014148
26. Feedback Instruments: 33-936s Digital Pendulum Control Experiments Manual. Tech. rep. (2006)